Supplementary Information

Self-assembled RNA interference microsponges for efficient siRNA delivery

Jong Bum Lee, Jinkee Hong, Daniel K. Bonner, Zhiyong Poon, Paula T. Hammond*

*To whom correspondence should be addressed. E-mail: hammond@mit.edu

This PDF file includes:

Materials and Methods

Chemicals and DNA sequences

T7 RNA polymerase and Ribonucleotide Solution Mix were purchased from New England Biolabs (Beverly, MA) in pure form at a concentration of 50,000 units/ml and 80 mM, respectively. RNase Inhibitor (RNAsin Plus) was purchased from Promega (Madison, WI) at a concentration of 40 units/µl. Linear 25,000 g/mol (M_w) polyethyleneimine (PEI) was purchased from Polysciences Inc. (Warrington, PA). Other chemical reagents were purchased from Sigma Aldrich (St. Louis, MO). Oligonucleotides were commercially synthesized and PAGE purified (Integrated DNA Technologies, Coralville, Iowa). Sequences of the oligonucleotides are listed in Table S1. siRNA for control experiments was purchased from Dharmacon RNAi Technologies. Dual-Glo Luciferase Assay System was purchased from Promega (Madison, WI). All other cell culture reagents were purchased from Invitrogen. GFP- and Luciferase-expressing T22 cells were a gift of the laboratory of Phil Sharp (MIT). Vivo Tag 645 and Cyanine 5-dUTP was purchased from Visen/PerkinElmer.

Circularization of linear DNA.

0.5 µM of phosphorylated linear ssDNA (ATAGTGAGTCGTATTAACGTA CCAACAACTTACGCTGAGTACTTCGATTACTTGAATCGAAGTACTCAGCGTAA GTTTAGAGGCATATCCCT) was hybridized with equimolar amounts of short DNA strands containing the T7 promoter sequence (TAATACGACTCACTATAGGGAT) by heating at 95 ºC for 2 min and slowly cooling to 25 ºC over 1 hour. The circular DNA is synthesized by hybridizing a 22 base T7 promoter with a 92 base oligonucleotide which has one larger (16 bases) and one shorter (6 bases) complementary sequence to the T7 promoter (Table S1). The nick in the circular DNA was chemically closed by T4 DNA ligase (Promega, Madison, WI), following commercial protocol(1).

Gel electrophoresis

The resultant solution after dicer treatment of the RNA microsponges was run in a 3% agarose ready gel (Bio-Rad) at 100 V at 25 °C in Tris-acetate-EDTA (TAE) buffer (40 mM Tris, 20 mM acetic acid and 1 mM EDTA, pH 8.0, Bio-Rad) for 90min. The gel was then stained with 0.5 mg/ml of ethidium bromide in TAE buffer. The gel electrophoresis image was used to calculate the number of siRNA from RNA particle. By comparing the band intensity of cleaved 21bp RNA strands to standard RNA strands, the amount of siRNA, which was converted from RNAi microsponges, was calculated (Table S2). Although up to 460ng of siRNA can be theoretically obtained from 1μg of RNAi microsponges, the particles were experimentally converted to 94.5ng of siRNA by Dicer treatment under optimal conditions.

Dynamic Light Scattering (DLS) and Zeta Potential

The size and surface charge of RNAi microsponges were measured using Zeta PALS and Zeta Potential Analyzer software (Brookhaven Instruments Corp., Holtsville, NY). The RNAi microsponges were diluted in Milli-Q water and all measurement were carried out at 25 °C. Three measurements each with 10 sub-runs were performed for each sample. Molecular weight of RNA microsponges, 1.36×10^{10} g/mole, was obtained from Zeta PALS software.

Calculation of amount of siRNA generated from RNAi microsponges

From the measured molecular weight of the RNA microsponges, the number of periodically repeated 92 base RNA strands (from 92 base circular DNA templates) in a single RNA microsponge was calculated as follows:

- Molecular Weight of 92 base RNA strand = 28587 g/mole
- *Number of 92 base RNA strands (cleavable RNA strands) in one RNA microsponge* = $1.36 \times 10^{10} / 28587 = 4.76 \times 10^{5}$

In theory, 480000 of siRNA can be maximally generated from one RNAi microsponge. Experimentally, the amount of cleaved siRNA from one RNA microsponge was determined using the gel electrophoresis results.

- *siRNA from one RNA particle* = Amount of siRNA from 1μg of RNA microsponge / amount of 1 μg of RNA microsponge
  = (0.0945 μg / 12600 μg / mol) / (1 μg / 1.36 x 10^{10} μg / mol) = 102,000

According to gel electrophoresis results following the Dicer treatment, 102,000 siRNA strands were generated from one RNAi microsponge under optimal conditions.
This result shows that 21% of potential RNAi is converted as siRNA. In our hypothesis, some portion of the RNA is not as readily accessed by dicer in a more close-packed self-assembled RNA structure. Therefore, multimers such as dimer, trimer, and tetramer of repeat RNA unit as incomplete dicing products could be produce.

Calculation of amount of liposome by Lipofectamine with siRNA

The number of liposome can be calculated by the following equation,

$N_{liposome} = N_{lipid} / N_{tot}$

If 100 nm liposomes are unilamellar structure, the number of lipids in a 100 nm size liposome is about 80047 (references 1-3). With 2mg/ml of lipofectamine™ reagent (Invitrogen) solution, which is 3:1 (w/w) liposome formulation of DOSPA (2,3-dioleoyloxy-N- [2(sperminecarboxamido)ethyl]-N,N-dimethyl-1-propaniminium trifluoroacetate) and DOPE (dioleoyl-L-a-phosphatidylethanolamine), 1:4 ratio of siRNA/Lipo (w/v) is formed.

1. H. E. Hofland, L. Shephard, and S. M. Sullivan, Formation of stable cationic lipid/DNA complexes for gene transfer, Proc. Natl. Acad. Sci. USA, 93, 7305 (1996).
2. P. Shih, K. Evans, F. Lichaa, J. Lan, and P. Nelson, Focus, 19, 52 (1997).
3. P. Nelson, V. Ciccarone, J. Jessee, and P. L. Felgner, Focus, 15, 73 (1993).

Based on our calculation, about 150 times more number of liposomes that are made of lipofectamine agent are needed to deliver same number of siRNA in comparison to microsponges. For example, to deliver 1nmole of siRNA, 1.5 pmole of liposome is necessary (in case of RNAi-MS, about 10fmole of RNA-MS can deliver 1nmole of siRNA). This is critical issue for the cell type that does not easily allow cellular uptake and low off-target/toxicity [*Science*, 319, 627, (2008)].

Materials for *in vitro* Biological Characterization

The siRNA was purchased from Dharmacon RNAi Technologies. Dual-Glo Luciferase Assay System and Fugene-HD were purchased from Promega. All other cell culture reagents were purchased from Invitrogen. T22 cells stably expressing both GFP and firefly luciferase, untransfected T22 cells, and pRL-CMV (*Renilla* luciferase) plasmid were a gift of the laboratory of Phil Sharp (MIT). gWIZ-Luc (Firefly luciferase) plasmid was obtained from Aldevron. (Firefly) Branched 25,000 g/mol (M_w) polyethyleneimine (PEI) and other chemical reagents were purchased from Sigma Aldrich. Vivo Tag 645 was purchased from Visen/PerkinElmer.

Cell proliferation assay

T22 cells were seeded at 2000 cells/well in a 96-well clear, flat-bottomed plate and transfected according to the above protocol. Cells were incubated with RNAi-microsponges or RNAi-microsponge/PEI for 4 hours, after which media was removed and replaced with 10% serum-containing growth medium. After 48 hours, each well was treated with 20 μL of MTT reagent (1 mg/mL in aMEM) for an additional 4 hours. Media was then removed and formazan crystals were solubilized in 50:50 DMF:water with 5% SDS. After 12 hours, absorbance was read at 570 nm.

Cell uptake test by confocal microscopy

8-well Lab-Tek chamber slides (Thermo Fisher, Waltham, MA) were treated for 20 min with human fibronectin in PBS at 0.1 mg/mL. The fibronectin was removed and T22 cells were trypsinized and seeded in each well at a concentration of 4000 cells/well 24 h before transfection. 50 μL of fluorescently labeled RNAi-MS and RNAi-MS/PEI were added to 250 μL phenol-free Opti-MEM at the final concentration of up to 21.2fM. After 4 hours, RNAi-microsponges were removed, cells were fixed with 3.7% formaldehyde in PBS, stained with Hoechst 33342 (Pierce) and Alexa Fluor 488® phalloidin (Invitrogen) and washed 3 times with PBS. Imaging was done on a PerkinElmer Ultraview spinning disc confocal (PerkinElmer, Waltham, MA).

Materials for *In vivo* siRNA Knockdown Experiments. T22-Luc cells were a generous gift from Dr. Deyin Xing, Professor Philip Sharp (MIT) and Dr. Sandra Orsulic

(Cedars-Sinai medical center). Tumors from nude mice injected with Brca1 wild-type cell line C22 were used to generate T22 tumor cell lines (*Cancer Res*. 2006 Sept 15; 66(18): 8949-53). T22-Luc is a genetically defined mouse ovarian cancer cell line (p53-/-, Akt, myc) that stably expresses luciferase after infection with pMSCV-puro-Firefly luciferase viral supernatant and selecting the cells in a medium containing 2.0 μg/ml of puromycin for 1 week.

Degradation Experiments of RNAi microsponges.

For degradation test, RNA microsponges were incubated for 24 hrs in 10% of serum at 37 °C (Fig. S13). We have also carried out additional experiments with various concentrations of RNase for 24 hrs at 37 °C (Fig. S3) [RNase I (from 0.05U/μl to 5U/μl) for single stranded RNA and RNase III (from 0.02U/μl to 1.2U/μl) for double stranded RNA, NEB, Ipswich, MA]. As a control, RNA microsponges were incubated with 10U/μl of DNase I (NEB, Ipswich, MA) for 24 hrs at 37°C.

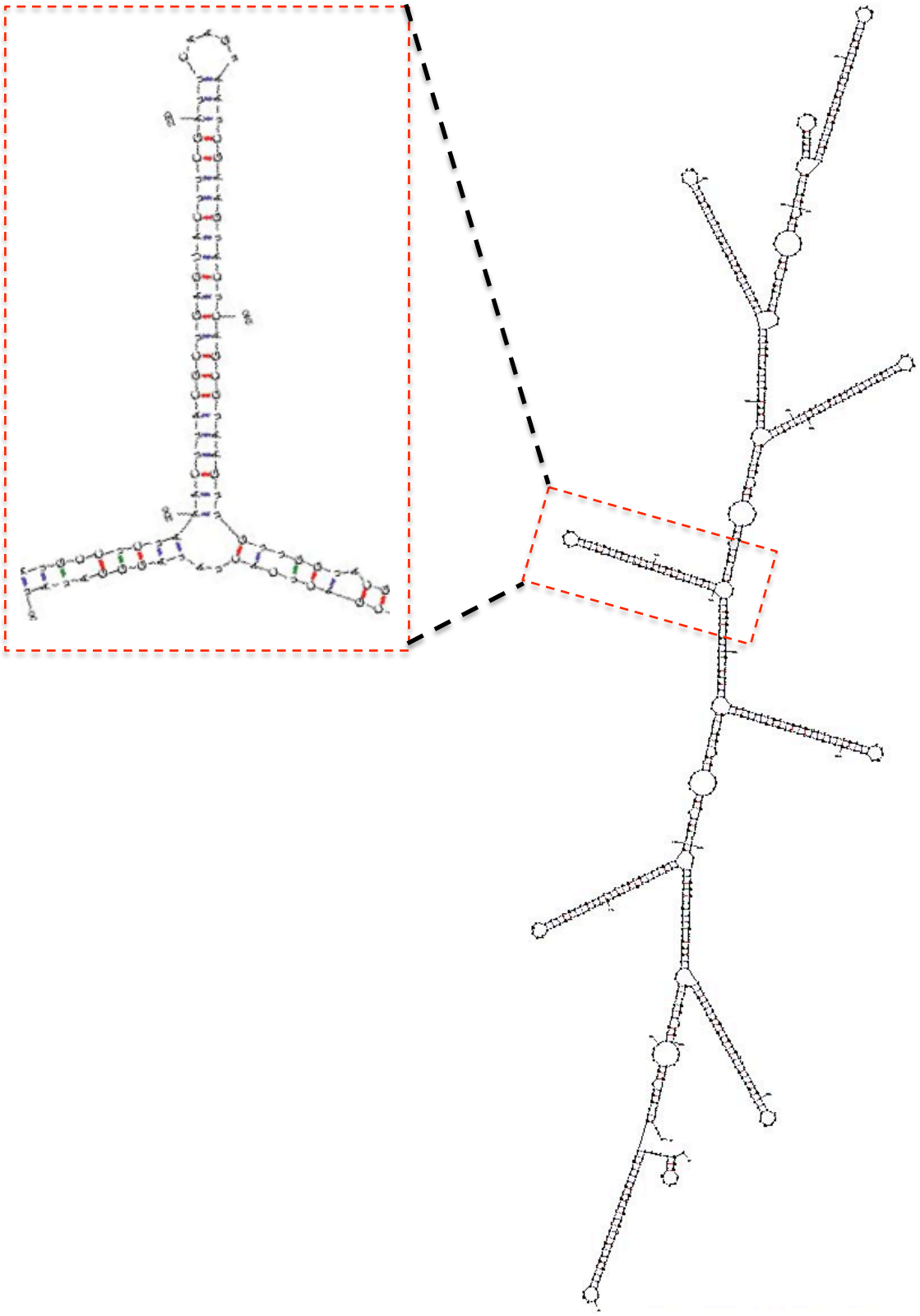

Figure S1. Secondary structure of eight repeated units produced by RCT (using M-fold software).

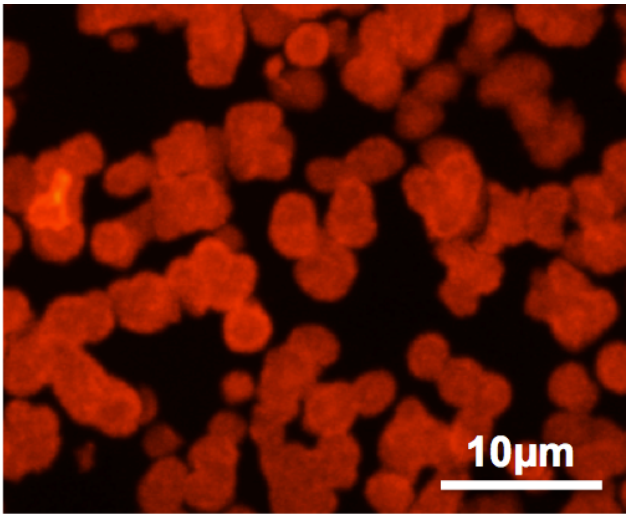

Figure S2. Confocal image of RNAi-microsponges labeled with Cyanine 5-dUTPs. RNAi polymerization took place with rolling circle transcription in the presence of Cyanine 5-dUTPs used as one of the ribonucleotides to form the RNA-microsponge. The red fluorescence from the RNAi-microsponge confirms that the microsponge is formed of RNA.

RNase	SEM Images
No RNase	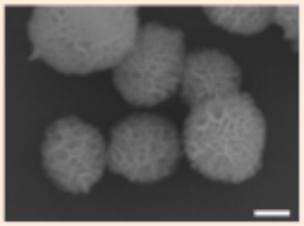
RNase I (0.05U/µl) Rnase III (0.02U/µl)	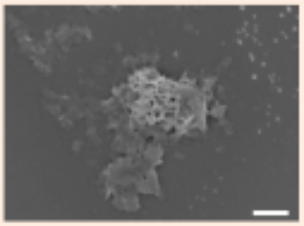
RNase I (0.2U/µl) Rnase III (0.08U/µl)	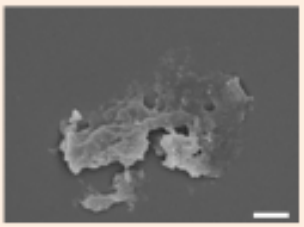
RNase I (1U/µl) Rnase III (0.4U/µl)	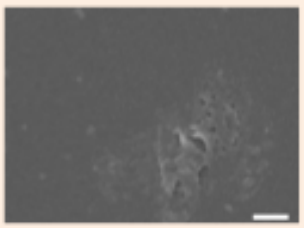
RNase I (5U/µl) Rnase III (1.2U/µl)	

DNase	SEM Images
DNase I (10U/µl)	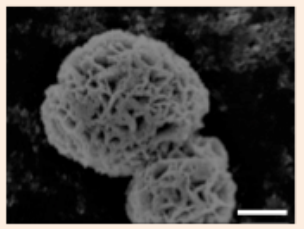

Figure S3. SEM images of RNAi-microsponges after incubation with various concentrations of RNase (RNase I for single stranded RNA and RNase III for double stranded RNA, NEB, Ipswich, MA). The degradation of RNA microsponge at different concentrations of RNase suggests that our microsponge is made of RNA. At lower concentrations, the size of microsponges is decreased but still protected from RNase. As the concentration increase, the microsponges is not able to maintain the particle form by degradation. Finally, RNA fragments of the microsponges are completely disappeared at the higher concentration of RNase. However, RNA microsponge is intact after incubation with high concentration of DNase I, suggesting that circular DNA is not the building material for microsponges. Scale bars indicate 1µm.

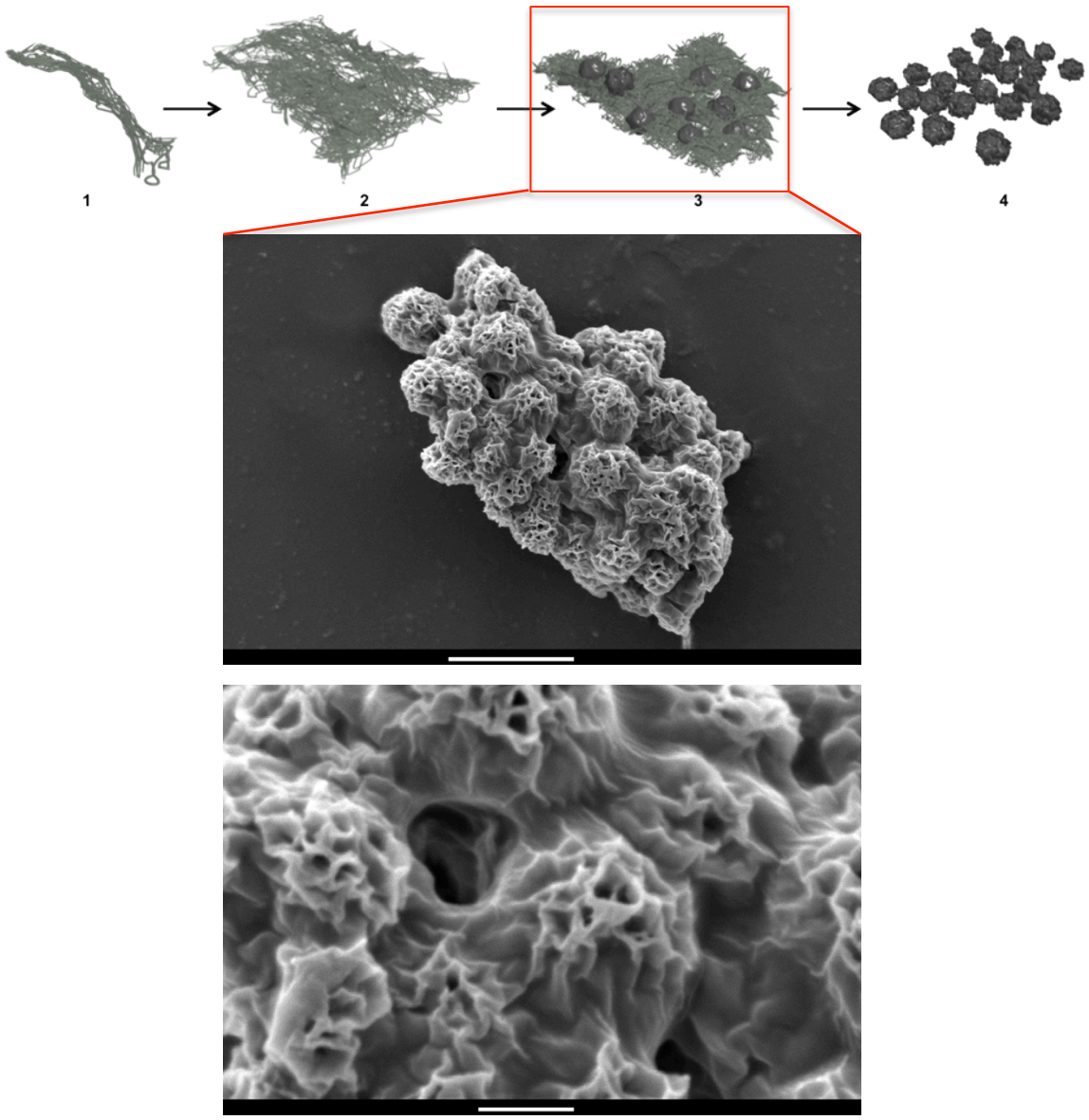

Figure S4. Cartoon schematic image of the formation of RNAi-microsponges (Top). Scanning electron microscope images of preliminary structure of RNAi-microsponges after 12h rolling circle transcription (Bottom). Scale bars indicate 5μm and 1μm.

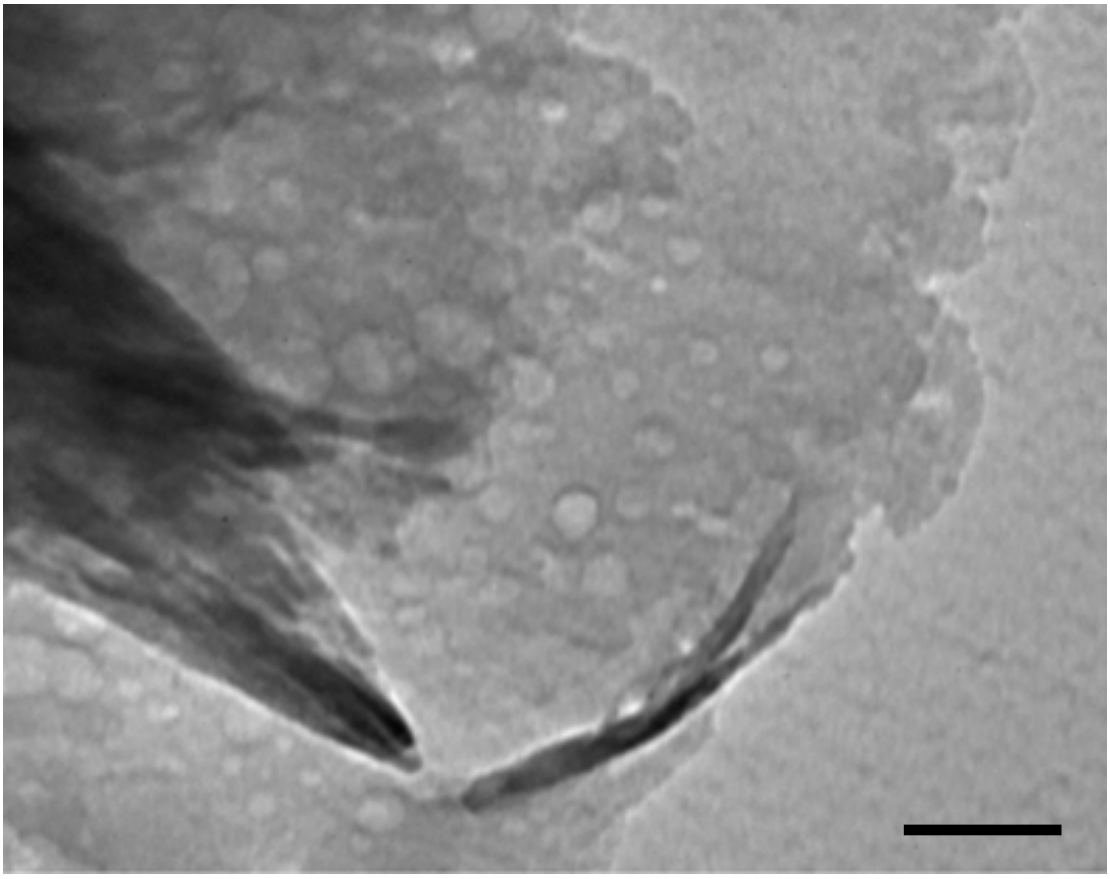

Figure S5. Transmission electron microscope image of RNAi microsponge. Multi-layered RNA sheets are shown in high magnification image. Scale bar indicates 50nm.

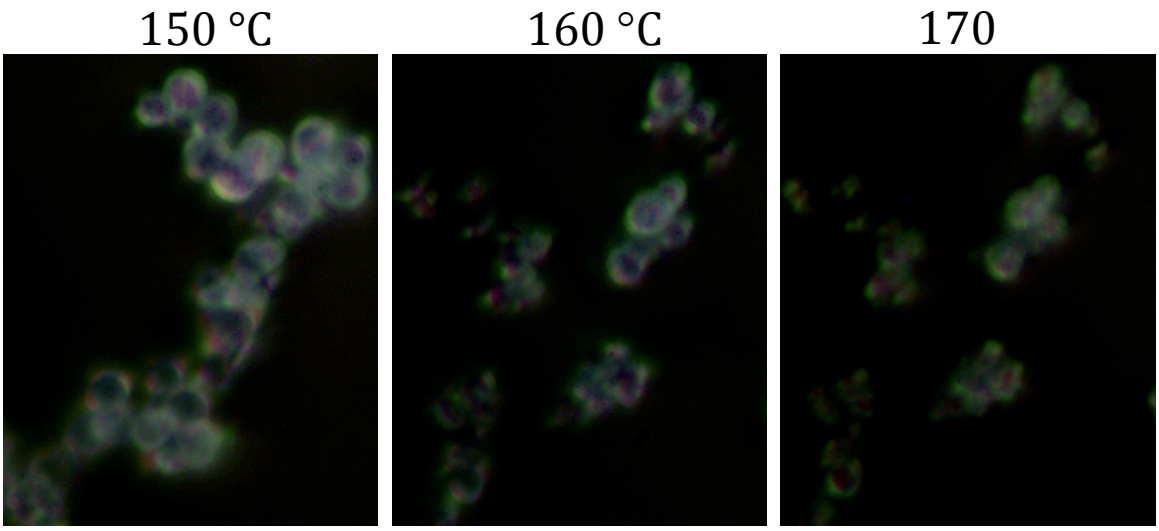

Figure S6.Polarized optical microscopy images of RNAi-MS with heating stage.

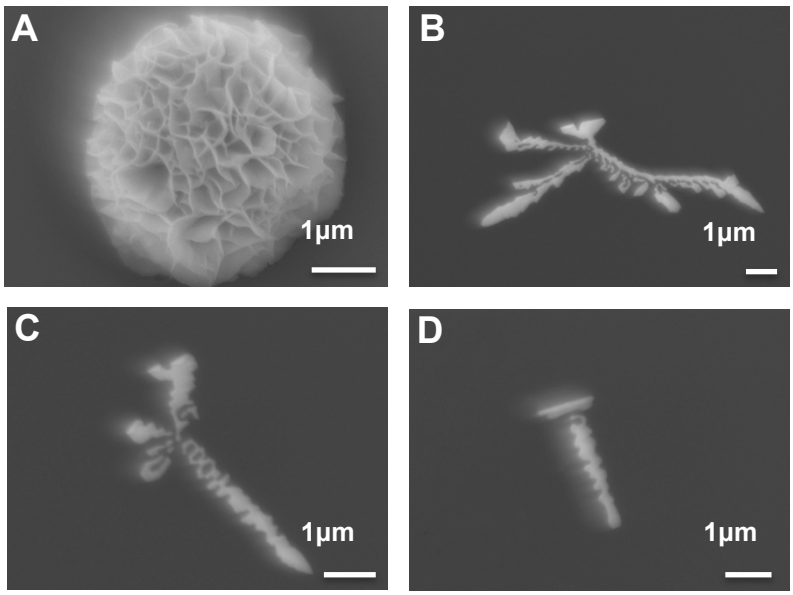

Figure S7. Scanning electron microscope images of RNA products by rolling circle transcription with different concentrations of circular DNA from 100nM (A), 30nM(B), 10nM(C), and 3nM(D). With 100 nM of circular DNA, sponge-like structures from RNA products are shown, however, microsponges are not generated with 30nM, 10nM, and 3nM of circular DNA. In figure B-D, RNA products form fiber-like structures that are similar to the products of time-dependent experiment after 1 hour RCT (see Fig 2A in main text). According to results from time dependent and concentration dependent experiments, we hypothesize that the mechanism of formation of RNAi-microsponge is crystallization of RNA polymers into thin lamellae by nucleation of poly-RNA when its concentration is higher than a critical concentration beyond which individual crystalline forms aggregate and merge into superstructures. Therefore, the final structure is reminiscent of the lamellar spherulite structures that are formed by highly crystalline polymers [Formation of Spherulites in Polyethylene. *Nature* **194**, 542-& (1962)].

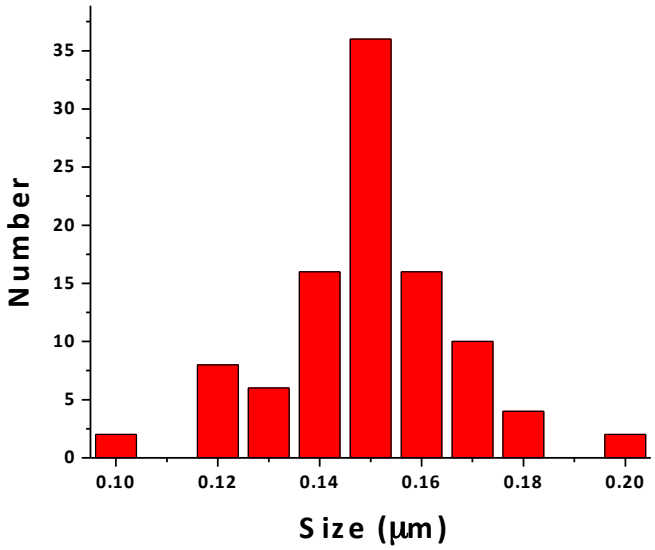

Figure S8. Distribution of the particle size of RNAi-microsponge/PEI.

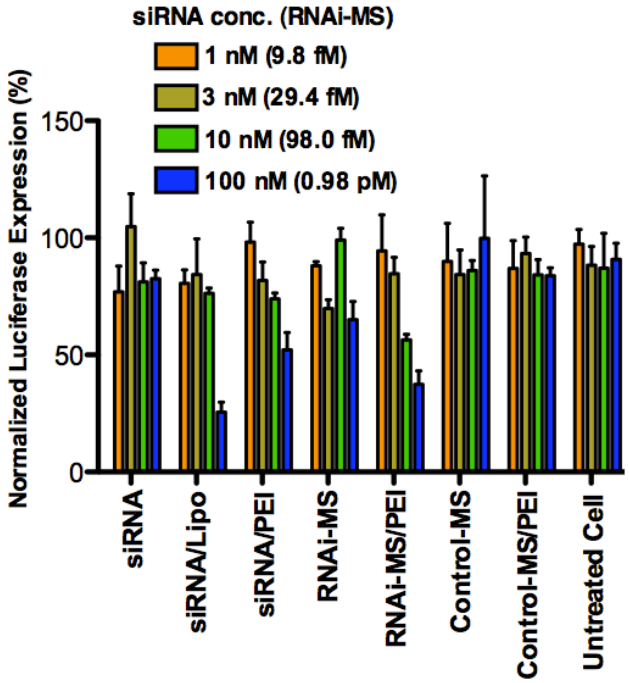

Figure S9. In vitro knockdown of luciferase by naked siRNA, siRNA/Lipo [siRNA/Lipofectamine (commercially available gene delivery reagent) complexes], siRNA/PEI, RNAi-MS, RNAi-MS/PEI, control-MS (RNA microsponge without meaningful sequence), control-MS/PEI, and untreated cell. The results show that any significant decrease of luciferase expression is not observed by control-MS and control-MS/PEI, supporting that there is no non-specific gene regulation in our experiments.

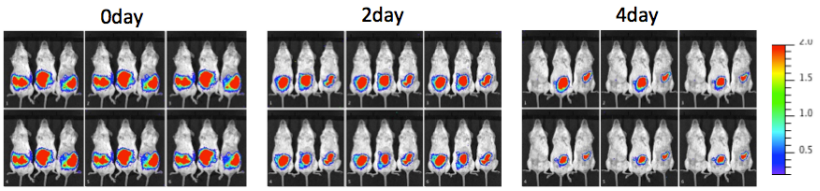

Figure S10. *In vivo* knockdown of firefly luciferase by RNAi-MS/PEI. Optical images of tumours after intratumoral injection of RNAi-MS/PEI into the tumor of mouse with six different wavelength.

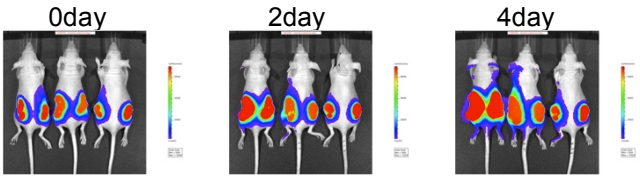

Figure S11. *In vivo* knockdown of firefly luciferase by control RNA microsponge/PEI. Optical images of tumours after intratumoral injection of control RNA microsponge/PEI into the tumor of mouse. Here, control RNA microsponge dose not contain siRNA for luciferase. A significant decrease of expression is not observed.

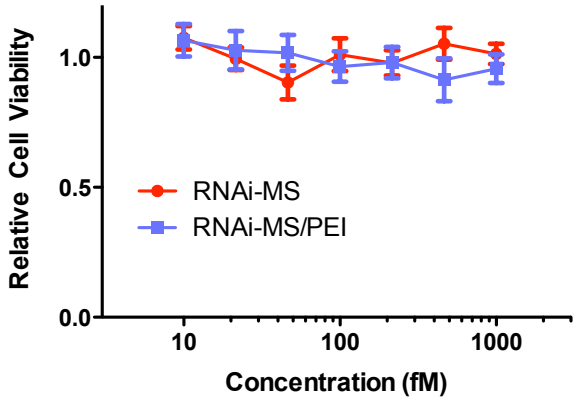

Figure S12. Cell viability assay of RNAi-microsponges

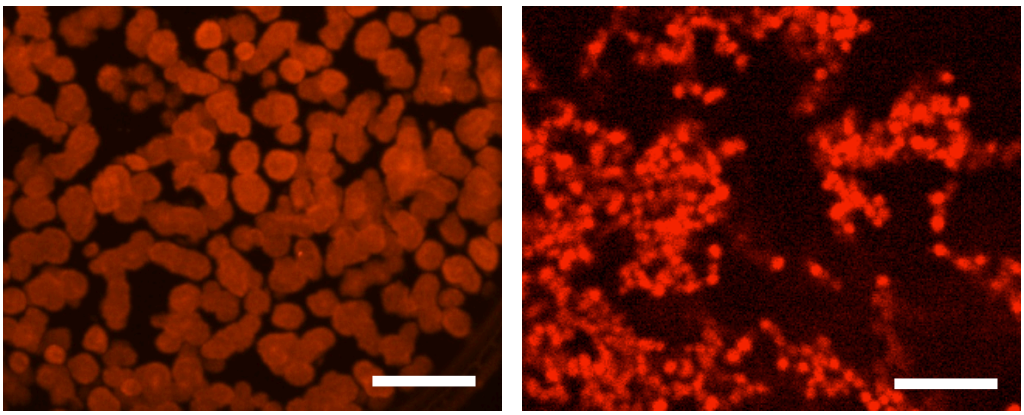

Figure S13. Fluorescence microscopic images of RNAi-microsponge before (left) after incubating in 10% Serum for one day at 37 °C (right). Scale bar indicates 10μm. The size of the RNAi-microsponge is reduced, possibly by degradation of RNAse, but still maintain the particle structure, supporting the idea that the RNA in the RNAi-microsponges are protected from degradation within the sponge structure.

Supporting Tables

Table S1. Oligonucleotide sequences of linear ssDNA and T7 promoter.

Strand	Sequence
Linear ssDNA	5'-Phosphate-ATAGTGAGTCGTATTAACGTACCAACAACTTACGCTG AGTACTTCGATTACTTGAATCGAAGTACTCAGCGTAAGTTTAGAGG CATATCCCT-3'
Promoter	5'-TAATACGACTCACTATAGGGAT-3'

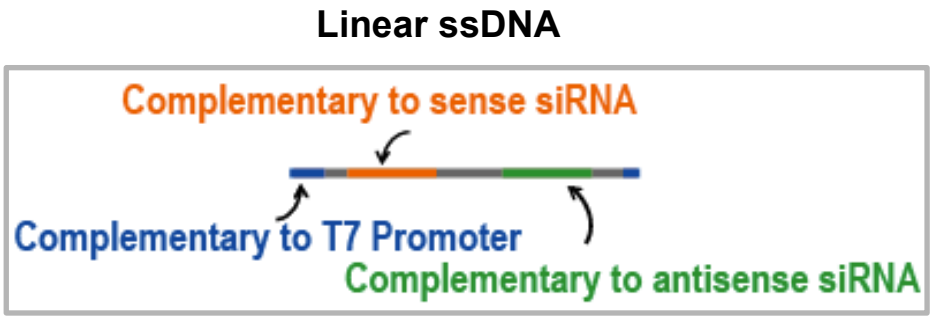

Table S2. Peak positions and d-spadings for RNAi-microsponge

Peak position, q[Å^{-1}]	**Spacing d[Å]**
0.57	11.00
1.18	5.32
1.77	3.56
2.16	2.91
1.04	6.02
2.08	3.03

Spacing was determined by Bragg's Law.

$$d = n\lambda / 2\sin\theta$$

Also, the scattering vector q was determined from the following equation.

$$q = 4\pi \sin\theta / \lambda$$

To determine the thickness of crystallite was determined from Scherrer's Formula.

$$D = 2\pi K/\Delta q$$

Here, K=0.9 is the Scherrer constant, and Δq is the radial full width at half maximum of a given Bragg spot. D is thickness of crystallite. λ is the wavelength of the x-ray radiation (here, λ is 1.54).

FWHM, Δq[Å^{-1}]	**Thickness of Crystallite, D[Å]**
0.077	73.3

Here, the crystallite thickness is estimated to be ~ 7.4 nm as determined from the Scherrer equation. The 7.4nm is close to the theoretical length of double stranded 21bp siRNA by considering that one base pair corresponds to 2.6 – 2.9 Å of length along the strand (21 x 2.6-2.9 = 54.6-60.9 Å). Considering that the polymer might fold according to the structure displayed Figure S1, the observed thickness might correspond to the length of a double stranded 21bp siRNA coupled to the width of a duplexed RNA helix of approximately 20 Å [*Nucleic Acids Research*, 27, 949-955 (1999)]. This would theoretically amount to 74.6 to 80.9 Å. In addition, the rest of RNA strands could be easily packing to form ordered structure since the persistence length of single-stranded RNA is less than 1nm. However, double stranded RNA part should be rigid because persistence length of double stranded RNA is about 64nm (Single-Molecule Measurements of the Persistence Length of Double-Stranded RNA, Biophys J. 2005 April; 88(4): 2737–2744).

Table S3. Amount of cleaved siRNA from 1µg of RNAi-microsponges from gel electrophoresis results.

	Intensity (abitrary)	**Std.**	**Amount (ng)**	
21 bp of dsRNA Ladder	**159.3**	**16.4**	**93.8 ± 9.7**	**Reference**
siRNA from RNA particles	**160.4**	**8.8**	**94.5 ± 5.2**	

References

1. S. Beyer, P. Nickels, and F. C. Simmel, *Nano lett*. **5**, 719 (2005).

2. D. Xing, S. Orsulic, *Cancer Res*. **66**, 8949 (2006).